ASAP1, a Gene at 8q24, Is Associated with Prostate Cancer Metastasis

Dong Lin,[1] Akira Watahiki,[1] Jane Bayani,[6] Fang Zhang,[1] Lin Liu,[2] Victor Ling,[2] Marianne D. Sadar,[3] John English,[4] Ladan Fazli,[5] Alan So,[5] Peter W. Gout,[1] Martin Gleave,[5] Jeremy A. Squire,[6] and Yu-Zhuo Wang[1,5]

Departments of [1]Cancer Endocrinology and [2]Cancer Genetics and [3]Genome Sciences Centre, British Columbia Cancer Agency; [4]Department of Pathology and [5]Prostate Centre at Vancouver General Hospital and University of British Columbia, Vancouver, British Columbia, Canada; and [6]Ontario Cancer Institute, Princess Margaret Hospital, Toronto, Ontario, Canada

Abstract

Metastatic prostate cancer is a terminal disease, and the development of reliable prognostic tools and more effective therapy is critically important for improved disease survival and management. This study was aimed at identifying genes that are differentially expressed in metastatic and nonmetastatic prostate cancer cells and, as such, could be critical in the development of metastasis. Long-SAGE analysis was used to compare a transplantable human metastatic prostate cancer subline, PCa1-met, with a nonmetastatic counterpart, PCa2. Both sublines were developed from a patient's prostate cancer specimen via subrenal capsule grafting and subsequent orthotopic implantation into SCID mice. Among various differentially expressed genes identified, ASAP1, an 8q24 gene encoding an ADP-ribosylation factor GTPase-activating protein not previously associated with prostate cancer, was up-regulated in the metastatic subline as confirmed by quantitative real-time PCR. Immunohistochemistry of xenograft sections showed that cytoplasmic ASAP1 protein staining was absent or weak in benign tissue, significantly stronger in nonmetastatic PCa2 tissue, and strongest in PCa1-met tissue. In clinical specimens, ASAP1 protein staining was elevated in 80% of primary prostate cancers and substantially higher in metastatic lesions compared with benign prostate tissue. Moreover, additional ASAP1 gene copies were detected in 58% of the primary prostate cancer specimens. Small interfering RNA–induced reduction of ASAP1 protein expression markedly suppressed in vitro PC-3 cell migration (~50%) and Matrigel invasion (~67%). This study suggests that the ASAP1 gene plays a role in prostate cancer metastasis and may represent a therapeutic target and/or biomarker for metastatic disease. [Cancer Res 2008;68(11):4352–9]

Introduction

Prostate cancer is the most common cancer, as well as the second leading cause of cancer-related deaths, for North American males. Once prostate cancer has metastasized, it is incurable, and most deaths from this disease are due to metastases that are highly resistant to conventional therapies. Metastatic prostate cancer is hence a terminal disease, and development of new therapeutic targets, as well as reliable biomarkers for detection of metastatic potential in primary tumors, is of critical importance for improved disease survival and management (1–3).

Metastasis is a multistep process thought to be based on changes in expression of specific genes (4). In view of this, changes in the expression of certain genes may serve as metastatic biomarkers and/or new targets for therapy of metastatic disease (2). Although many efforts have been made toward identification of metastatic biomarkers for prostate cancer (2, 3, 5, 6), few prognostic assays have thus far been submitted to the U.S. Food and Drug Administration (7). This is largely due to a lack of optimal models for studying the development of prostate cancer metastasis. Whereas established prostate cancer cell lines representing different stages of tumor progression can be useful for identifying mechanisms underlying metastasis and development of novel therapeutics, they do not adequately mimic clinical disease (8, 9). Efforts have therefore focused on models based on prostate cancer specimens from patients. However, the typical heterogeneity of such specimens, consisting of both nonmetastatic and metastatic subpopulations, makes it difficult to identify genes with critical roles in the development of metastasis (10, 11). To overcome such hurdles, we have recently developed an experimental prostate cancer model that not only resembles the clinical situation, but also allows establishment of transplantable prostate cancer sublines that differ in metastatic ability and, as such, can be useful for investigating development of metastasis at the molecular level. Our model is based on subrenal capsule grafting of a patient's primary prostate cancer tissue into immunodeficient mice leading to transplantable, heterogeneous tumor lines retaining major growth and histopathologic features of the original cancer (12). Metastatic sublines can be established from metastases that develop after orthotopic grafting of the tumor lines. Using this approach, we generated a metastatic subline, designated PCa1-met, whose orthotopic grafting into immunodeficient mice led to metastases in multiple common target organs, including lymph nodes, liver, and notably bone (11).

In the present study, we have established a nontissue-invasive and nonmetastatic prostate cancer subline, PCa2, from the same patient's specimen that gave rise to the metastatic PCa1-met subline. Using a modified version of Serial Analysis of Gene Expression (SAGE), i.e., LongSAGE (13), we compared orthotopically grown xenografts of the two closely related sublines with a view to identifying genes that were differentially expressed and, as such, could play a role in the development of metastatic ability. A number of differentially expressed genes were identified, including genes previously reported to have a role in tissue invasion and metastasis of prostate cancer cells. Differentially expressed genes

that had not previously been associated with prostate cancer were also identified, including *ASAP1* (*AMAP1/DDEF1*), a gene encoding an ADP-ribosylation factor (Arf) GTPase-activating protein recently reported to have a role in breast cancer–invasive activities (14). Evidence is presented that highly increased expression of ASAP1 protein in experimental and clinical prostate cancer specimens correlates with metastatic behavior. Furthermore, small interfering RNA (siRNA)–induced reduction of ASAP1 protein expression in PC-3 human prostate cancer cells was found to lead to markedly reduced cell migration and Matrigel invasion *in vitro*. The data suggest that the *ASAP1* gene plays a role in prostate cancer metastasis.

Materials and Methods

Materials and animals. Chemicals, stains, solvents, and solutions were obtained from Sigma-Aldrich Canada Ltd., unless otherwise indicated. NOD-SCID mice (ages 6–8 wk) were bred by the British Columbia Cancer Research Centre Animal Resource Centre, British Columbia Cancer Agency.

Xenografts. The patient-derived prostate cancer tissue line and its sublines were maintained by serial transplantation of subrenal capsule xenografts into male NOD-SCID mice supplemented with testosterone (10 mg/mouse), as previously described (11). Animal care and experiments were carried out in accordance with the guidelines of the Canadian Council on Animal Care.

Development of nonmetastatic prostate cancer sublines. Pieces of a prostate cancer xenograft were grafted under the kidney capsules of testosterone-supplemented male NOD/SCID mice, as previously described (11). Sections of grafted tissue, growing immediately under the capsule (i.e., farthest from the kidney cortex), were harvested and cut into pieces of ∼2 mm³. These pieces were regrafted into NOD-SCID mice under the kidney capsules (two per mouse). After five serial transplantations carried out in this manner, xenograft tissue was grafted into anterior prostates of mice. About 6 to 8 wk later, the hosts were sacrificed and examined for metastases of human origin in lymph nodes, lungs, liver, kidneys, spleens, and bone (femur). Tumor sublines devoid of metastatic activity during the 6-wk to 8-wk period, and further serial transplantation were considered nonmetastatic.

SAGE library construction and comparative analysis. Total RNA was extracted from orthotopically grafted PCa1-met and PCa2 tissues (16th generations) using an RNeasy mini kit (Qiagen). SAGE libraries were constructed using an I-SAGE kit (Invitrogen). The libraries' clones were sequenced by the British Columbia Genome Sciences Centre (BCGSC). Sequenced tags of the two tumor sublines were analyzed using Discovery-Space, a BCGSC-developed SAGE gene expression analysis software tool.[7] The tags were filtered by Experimental SAGE Tags Quality (DiscoverySpace) and annotated using the human and mouse gene and genome data CMOST integrated database. Because the transplantable xenograft tissues contain both human (tumor) and mouse (stroma) tissue, the SAGE tags were categorized as human-specific, mouse-specific, shared by human and mouse, and unannotated. In the present study, only human-specific tags were analyzed. Audic-Claverie *P* statistics (DiscoverySpace) was used to establish whether differences found for selected tags between PCa1-met and PCa2 tissues were statistically significant. Each ratio of the tag was calculated from frequencies per 100,000 human tags.

Quantitative real-time PCR. Total RNA was isolated from xenograft tissues using the RNeasy mini kit (Qiagen, Inc.) following the manufacturer's suggestions. The quality of the RNA samples was analyzed using Agilent Bioanalyzer (Agilent Technologies). RNA (1 μg) was treated with 0.5 units DNase I (amplification grade; Invitrogen) and then annealed with 50 ng random hexamer oligonucleotide. The cDNA was synthesized using the Superscript first strand synthesis system for real-time PCR (RT-PCR;

Invitrogen) following the manufacturer's suggestions. The cDNA products were diluted 20-fold before PCR amplification. Expression of selected genes was analyzed using a 7900HT Sequence Detection System (Applied Biosystems, Inc.). The quantitative RT-PCR (qRT-PCR) reaction was carried out in a 10-μL volume using cDNA (converted from 2.5 ng total RNA), a 150 nmol/L gene-specific primer pair, and Platinum SYBR Green qPCR SuperMix-UDG with ROX (Invitrogen). Duplicate reactions were performed for each sample, and data were averaged and normalized to a geometric mean of the expression of two housekeeping genes, *hprt* and *K-α1*, reported to be stably expressed in prostate tissue (15). Gene expression data are presented as fold change of one subline relative to the other subline. Because the xenograft samples consisted of both human and mouse cells, the following human-specific primers were designed for the *ASAP1, hprt* and *K-α1* genes, to ensure that only human cDNA, and not mouse cDNA, was amplified in qRT-PCR reactions: *ASAP1*, forward 5′-CCCCTTTTGCAG-CAACTTACA and reverse 5′-TCCTATGTCCCACAGTAAGCTGG; *hprt*, forward 5′-GGTCAGGCAGTATAATCCAAAG and reverse 5′-CGATGTCAA-TAGGACTCCAGAT; *K-α1*, forward 5′-GAGGTTGGTGTGGATTCTGTT and reverse 5′-AGCTGAAATTCTGGGAGCAT. Gene expressions are expressed as mean ± SD.

Clinical prostate cancer tissues. Specimens were obtained from patients, with their informed consent, following a protocol approved by the Clinical Research Ethics Board of University of British Columbia (UBC) and British Columbia Cancer Agency. Tissue microarrays (TMA) were constructed (16), at the Prostate Centre, Vancouver General Hospital (VGH), of 10 benign prostatic hyperplasia (BPH) and 66 paraffin-embedded radical prostatectomy specimens from randomly selected cancers (Department of Pathology, VGH/UBC) that had not been subjected to neoadjuvant hormone therapy. Areas with sufficient amounts of carcinoma and normal prostatic epithelium in the original, diagnostic H&E-stained tissue sections were identified by a pathologist. Using a Tissue Microarrayer (Beecher Instruments), four tissue cores were taken from each BPH and malignant specimen for TMA construction. In addition, sections from 11 lymph node, 2 lung, and 5 bone metastatic prostate cancers were obtained for ASAP1 protein analysis.

Immunohistochemistry. Preparation of paraffin-embedded tissue sections and immunohistochemical analyses were carried out as previously described (11). For ASAP1 protein analysis, rabbit polyclonal anti-ASAP1 antibody (Abcam) was used. All tissue sections were lightly counterstained with 5% (w/v) Harris hematoxylin. Control sections were processed in parallel with rabbit nonimmune IgG (Dako) used at the same concentrations as the primary antibodies.

ASAP1 scoring. Cytoplasmic and plasma membrane–associated ASAP1 protein staining in tissue samples was evaluated by two independent pathologists in blinded analyses. Specimens were graded from 0 to +3 intensity to represent a range from no staining to heavy staining. The localization of ASAP1 expression in benign and malignant prostate cells was also indicated. For statistical analysis, the Student's *t* test was used to compare mean ASAP1 protein expressions in normal and malignant prostate tissue sections. The analyses were performed on the mean value of ASAP1 protein expression for each specimen. Data obtained with *P* values of <0.05 were considered statistically significant.

Spectral karyotyping analysis. The analysis was carried out as previously described (11).

Fluorescence *in situ* hybridization analysis for determination of *ASAP1* gene copy number. Dual-color fluorescence *in situ* hybridization (FISH) karyotypic analysis of paraffin-embedded tumor tissue (5-μm sections) was performed, as previously described (17). To determine *ASAP1* gene copy numbers, two bacterial artificial chromosome (BAC) clones (RP11-582G12 and RP11-140N11) containing specific *ASAP1* sequences were used; chromosome 8 was identified using a CEP 8 centromere probe. BAC DNAs were extracted by standard methods and labeled with Spectrum Orange (Abbott Molecular, Inc./Vysis, Inc.). The chromosome localization and sequence identity of the BAC clones was confirmed by normal metaphase FISH and PCR analyses.

Cell cultures. Human PC-3 and LNCaP prostate cancer cell lines were obtained from American Type Culture Collection. Cultures were maintained

---

[7] http://www.bcgsc.ca/bioinfo/software/discoveryspace/

in RPMI 1640 supplemented with 10% fetal bovine serum (FBS), 100 IU/mL penicillin G, and 100 μg/mL streptomycin using regular culture conditions.

siRNA and cell transfection. Stealth RNA interference (RNAi) targeting *ASAP1* and negative control (scrambled) siRNAs were purchased from Invitrogen. The *ASAP1*-targeting Stealth RNAis were siRNA1, 5′-GACCA-GAUCUCUGUCUCGGAGUUCA-3′ and 5′-UGAACUCCGAGACAGAGAU-CUGGUC-3′ and siRNA2, 5′-GGGCAAUAAGGAAUAUGGCAGUGAA-3′ and 5′-UUCACUGCCAUAUUCCUUAUUGCCC-3′. Vehicle and scrambled siRNAs were used as controls. The scrambled sequences were 5′-GAUCGCAGAU-GUUUCUCGCUCGACA-3′ and 5′-UGUCGAGCGAGAAACAUCUGCGAUC-3′. To examine the effect of the siRNAs on *ASAP1* expression, PC-3 cells were plated in six-well plates in antibiotic-free RPMI 1640. After 20 h, the cells were transfected with 60 nmol/L siRNA in Lipofectamine 2000 reagent following the manufacturer's instructions. Briefly, a complex of Lipofect-amine 2000 and siRNA in Opti-MEM (500 μL) was gently added to each well. After 8 h, the transfection mixture was removed and fresh antibiotic-free RPMI 1640 was added. Vehicle (Lipofectamine 2000) and scrambled siRNA were applied in separate wells. After 72 h incubation, the PC-3 cells were used for Western blot analysis and cell invasion and scratch wound healing assays.

Western blotting. PC-3 cell lysates were prepared using cell lysis buffer supplemented with a protease inhibitor cocktail (Roche); total lysate protein was determined using the bicinchoninic acid protein assay (Pierce). Typically, 5 μg whole-cell lysates were run on 7.5% SDS polyacrylamide gel for Western blotting, as previously described (11). Mouse anti-ASAP1 monoclonal antibody (BD Biosciences) was used as a primary antibody.

Scratch wound healing migration assay. PC-3 cells were seeded into six-well culture plates using their regular maintenance medium. After the cells had reached confluence, the medium was removed and a plastic pipette tip was drawn across the center sections of the wells to produce clean ∼1-mm-wide open areas (wounds) in the monolayers. Photographs were taken immediately and after 24 h of further incubation at 37°C in RPMI 1640 with reduced serum content (0.1% FBS). The cell-recovered areas at 24 h were measured to estimate the extent of cell migration (18). Percentage wound healing data are expressed as means ± SD.

Cell invasion assays. The assays were performed using modified Boyden chambers consisting of 8-μm pore filter inserts in 24-well plates (BD Biosciences), as described elsewhere (19). PC-3 cells in serum-free RPMI

1640 were plated (7.5 × 10^4 per well) on Matrigel-coated and uncoated membranes of the upper compartments and incubated at 37°C in a CO_2 incubator, using 5% FBS in the lower chambers as a chemoattractant. After 22 h, the inserts were pulled out and the noninvading cells on the upper surface were removed with a cotton swab. The cells on the lower surface of the membrane were fixed in methanol, air-dried, and stained with 0.1% crystal violet for 10 min. The cells on each membrane were counted in five fields (at 200× magnification) using a light microscope. Tumor cell invasion was expressed as the percentage of cells that had passed through the Matrigel-coated membranes relative to the number of cells that had passed through the uncoated membranes (invasion index). Results from triplicates are expressed as means ± SD.

Results

Development of a nonmetastatic prostate cancer subline. A transplantable, nontissue-invasive, nonmetastatic subline, designated PCa2, was derived from subrenal capsule xenografts of the same cancer specimen used to develop the metastatic PCa1-met subline (ref. 11; Fig. 1). The human origin of the PCa2 subline was confirmed by immunohistochemistry using antihuman androgen receptor, antiprostate-specific antigen antibodies (data not shown), and antihuman mitochondria antibody (Fig. 1*B*). The tumor volume doubling time of PCa2 xenografts in testosterone-supplemented mice was ∼5 days, approximating that of the PCa1-met subline. The PCa2 subline also resembled the PCa1-met subline with regard to poor cellular differentiation. Grafting of the PCa2 subline into anterior mouse prostates (the orthotopic site) showed a 100% take rate. However, in contrast to the PCa1-met subline, the PCa2 subline did not invade prostatic smooth muscle tissue of the host (Fig. 1*A* and *B*). Furthermore, H&E staining and immunohistochemical analysis indicated that there were no metastases in lymph nodes, lung, liver, kidney, spleen, and bone of mice bearing orthotopic PCa2 xenografts even after 8 weeks of grafting. This is in sharp contrast to the metastatic spread of orthotopically grafted PCa1-met tissue in mice previously observed
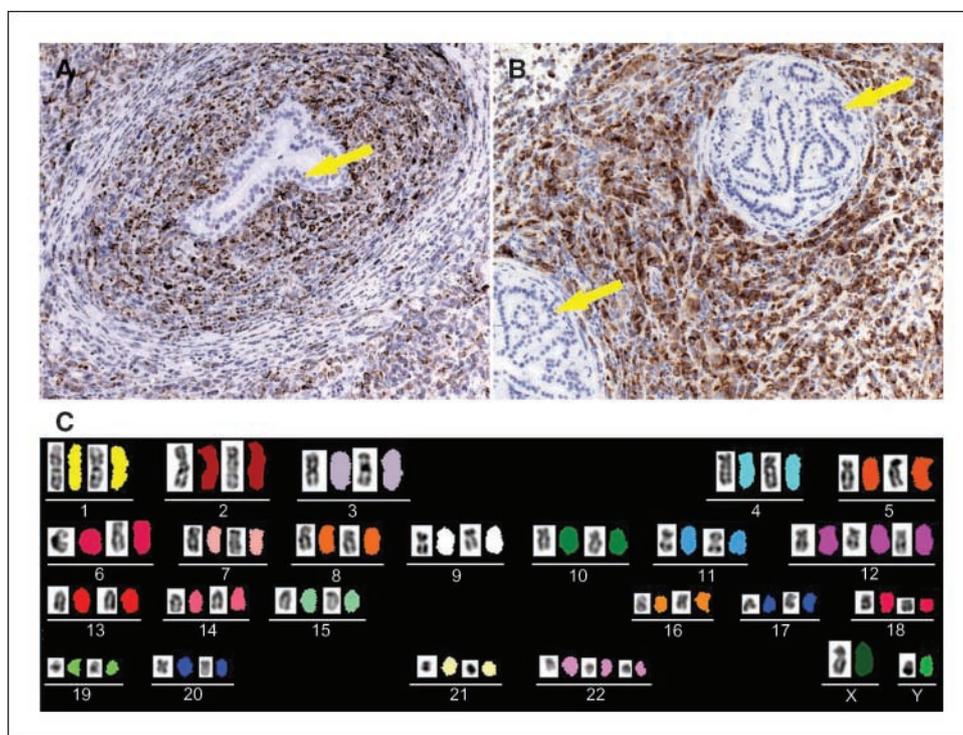

Figure 1. Tissue sections showing (*a*) differences in host tissue invasiveness between PCa1-met and PCa2 orthotopic xenografts during an 8-wk assay and (*b*) human origin of the cancer cells; SKY karyotype of the PCa2 subline. PCa1-met cells (*A*) and PCa2 cells (*B*) are positively stained with antihuman mitochondria antibody in contrast to prostatic ductal epithelial cells of the mouse host. Immunohistochemistry staining shows that PCa1-met cells have penetrated smooth muscle surrounding a mouse host prostatic duct (*arrow*) and grown around it (*A*) and that, in contrast, host tissue is apparently not invaded by PCa2 cells (*B*). *C,* SKY image from a representative metaphase spread of PCa2 tumor tissue with the classified colors and inverted 4′,6-diamidino-2-phenylindole. Clonal gain of chromosomes 12 and 22 was detected; no structural rearrangements were observed.

Figure 2. ASAP1 protein expression shown by immunohistochemistry in tissue sections of xenografts of benign and malignant prostate tissues all originating from the same patient's prostate cancer specimen. *A,* nonmetastatic PCa2 cells showing moderate cytoplasmic expression. *B,* metastatic PCa1-met cells showing strong cytoplasmic expression of the ASAP1 protein. *C,* benign prostate tissue showing weak cytoplasmic and moderate plasma membrane–associated expression of ASAP1. *D,* slow-growing prostate cancer grafts showing moderate cytoplasmic expression of ASAP1. Original magnifications, 200× (except insert in *C,* 400×).
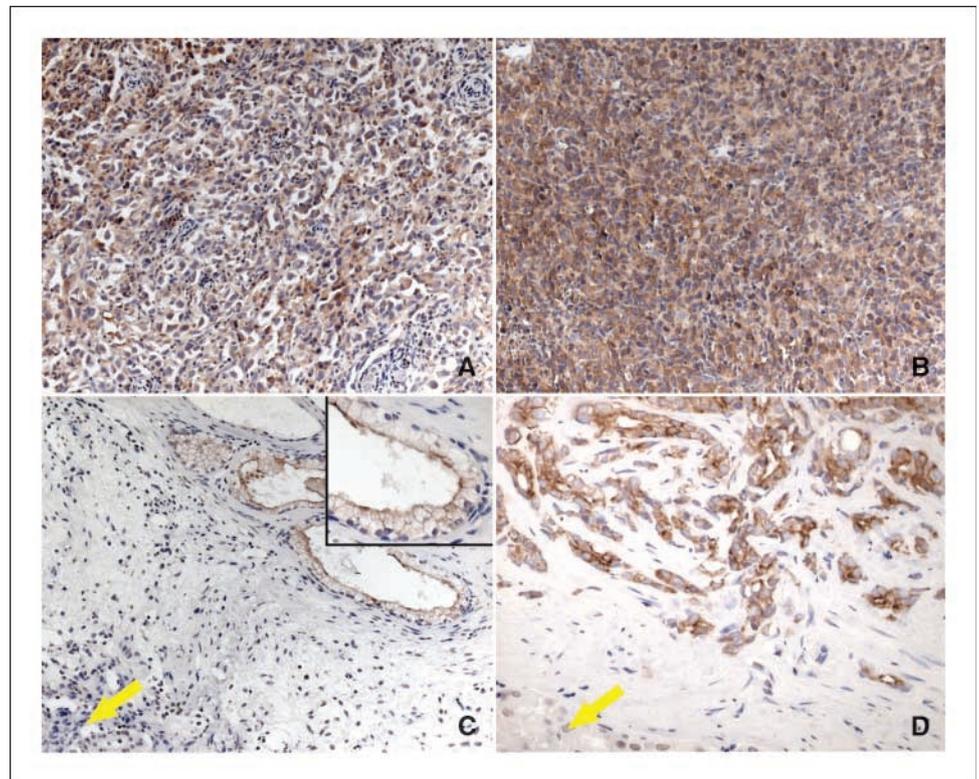
during an 8-wk period (11). The data show that the PCa2 subline, relative to the PCa1-met subline, can be considered nonmetastatic. Furthermore, the Spectral karyotyping analysis (SKY) karyotype of the PCa2 subline (Fig. 1*C*) is similar to that of the PCa1-met subline (11). It only differed in a few aspects, including gain of chromosomes 12 and 22 and absence of structural rearrangements, such as the translocation and deletion observed in the PCa1-met subline. It may be noted that the chromosome numbers of the two sublines do not deviate much from the normal number. As a pair, the PCa1-met and PCa2 sublines seem to provide a useful means for differentiating cellular and molecular genetic mechanisms involved in the metastatic process, especially because both were derived from one patient's cancer specimen. Notably, by using xenografts of the sublines at the orthotopic graft site, a microenvironment was provided similar to that of the original cancer.

Comparative analysis of SAGE libraries from metastatic and nonmetastatic prostate cancer sublines. Tissues from PCa1-met and PCa2 sublines, maintained as xenografts in mice, were grafted orthotopically (16th generation) and, after seven tumor volume doublings, harvested for SAGE. LongSAGE libraries of the PCa1-met and PCa2 sublines were developed, containing 128,409 and 127,005 tags, respectively. Mapping of the tags to a Reference Sequences database (RefSeq) revealed that 87,070 of the PCa1-met tags and 64,666 of the PCa2 tags were of human origin. DiscoverySpace analysis of these tags indicated that the PCa1-met library, relative to the PCa2 library, contained 220 differentially expressed known human genes, i.e., 135 genes were significantly up-regulated and 85 genes were down-regulated (*P* < 0.05). Some of these differentially expressed genes have previously been reported to play a role in prostate cancer with regard to tissue invasion and metastasis, including *CD44* (20), *E-cadherin* (21, 22), *CXCR4* (23), *caveolin-1* (24), *c-Met* (25), and *ETV6* (26). Of the differentially expressed genes not previously associated with prostate cancer, the *ASAP1* gene is of

particular interest, because its tags in the metastatic library (10.33/100,000) were found to be 6.7 times more prevalent than in the nonmetastatic library (1.55/100,000; *P* = 0.038) and it had been linked to metastatic activity of breast cancer (14).

Differential *ASAP1* gene expression in PCa1-met and PCa2 tumor sublines. To validate differential *ASAP1* expression in the PCa1-met and PCa2 tumor sublines, expression of the *ASAP1* gene was measured using qRT-PCR in samples of the two sublines derived from 12th, 14th, and 16th generations harvested at 27 to 35 days postgrafting. The *ASAP1*-mRNA levels were significantly higher in the metastatic PCa1-met than in the nonmetastatic PCa2 subline, showing 2.3 ± 0.4, 2.3 ± 0.1, and 2.1 ± 0.3 fold differences in the 12th, 14th, and 16th generations, respectively (*P* < 0.001). The differential was essentially the same for the three generations examined, indicating that there was no major change in differential *ASAP1* gene expression through five consecutive passages of the sublines.

Differential expression of ASAP1 protein in xenograft tissues. Using immunohistochemistry, levels of ASAP1 protein were determined in xenografts of nonmetastatic PCa2 and metastatic PCa1-met tissue, as well as benign and slow-growing malignant tissue, all originating from the same patient's prostate cancer specimen. The PCa2 and PCa1-met sublines showed moderate and strong cytoplasmic staining for ASAP1 protein, respectively (Fig. 2*A* and *B*). The much stronger staining for ASAP1 protein in PCa1-met tissue compared with PCa2 tissue was consistent with the higher levels of *ASAP1*-mRNA found in the PCa1-met subline. ASAP1 protein was also detected in benign prostate tissue grafts (Fig. 2*C*) and slow-growing prostate cancer grafts (Fig. 2*D*), which had survived transplantation into testosterone-supplemented NOD-SCID mice, but did not show significant growth even after 6 months of grafting. In these cases, moderate ASAP1 protein expression was mainly associated with the plasma

membrane. Whereas the benign tissue showed weak or no cytoplasmic ASAP1 protein staining, the slow-growing malignant tumor grafts showed weak or moderate cytoplasmic ASAP1 protein staining, similar to that observed in the nonmetastatic PCa2 subline. In contrast to the benign tissues and slow-growing malignant tissues, the fast-growing PCa2 and PCa1-met tissues showed no staining associated with the plasma membrane. Taken together, the xenograft-derived data suggest that moderate or high cytoplasmic ASAP1 protein staining, coupled to absence of plasma membrane–associated ASAP1 protein, may be an indication of elevated growth rates of prostate cancer. In addition, highly elevated ASAP1 protein expression seems to be associated with metastatic potential.

Expression and subcellular localization of ASAP1 protein in clinical prostate samples. A TMA of clinical prostate samples, i.e., 10 BPH and 66 primary cancer tissues, was examined for ASAP1 protein expression. Nine of the 10 benign prostate tissues showed no or only weak ASAP1 protein expression in the cytoplasm with moderate expression of the protein at the plasma membrane (Fig. 3*A* and *B*), a finding consistent with the observations with benign prostate tissue xenografts (Fig. 2*C*). In 53 of the 66 prostate cancer tissues (80%), moderate to strong cytoplasmic ASAP1 protein expression was observed. The intensity of cytoplasmic ASAP1 protein staining in these prostate cancer tissues (2.1 ± 0.7; Fig. 3*C* and *D*) was significantly higher than in the benign tissues (0.9 ± 0.3; $P < 0.01$; Fig. 3*A* and *B*). Also, 51 cancer cases showed weak or absent plasma membrane–associated ASAP1 protein staining. The intensity of plasma membrane–associated ASAP1 protein staining in the prostate cancer tissues (0.8 ± 0.6) was significantly lower than that in the benign tissues (1.9 ± 0.2; $P < 0.01$; Fig. 3).

Individual-invasive and metastatic prostate cancer tissues, i.e., 11 lymph node, 2 lung, and 5 bone metastatic prostate cancer tissues, were also examined for ASAP1 protein expression. Strong ASAP1 expression was observed in perineural (data not shown) and vascular-invasive prostate cancers (Fig. 4*A*). In all metastatic prostate cancer tissues examined, the cytoplasmic ASAP1 expression (2.6 ± 0.6) was very high (Fig. 4*B–D*) and significantly stronger ($P < 0.01$) than in the primary prostate cancer tissues (Fig. 3). The data indicate that the differential ASAP1 protein staining of the clinical samples is consistent with that found with the model prostate tissue xenografts (Fig. 2).

***ASAP1* gain/amplification in clinical prostate samples.** To investigate whether increased ASAP1 protein expression correlated with gain or amplification of the *ASAP1* gene, two *ASAP1*-specific BAC probes were combined and used for interphase FISH analysis of 18 benign and 38 primary prostate cancer samples. Chromosome 8 was identified using a CEP 8 centromere probe. As expected, the 18 benign prostate tissues did not show any increase in *ASAP1* copy number per cell (data not shown). In contrast, there was a significant increase in *ASAP1* copy number in 22 of the 38 primary prostate cancer cases (58%). Among these 22 cases, 21 cases showed *ASAP1* gain resulting from polysomy of chromosome 8, i.e., 20 cases showed low-level gain (three to four copies of *ASAP1* per cell; Fig. 5*A*), whereas one showed a high copy number gain (five copies or more of *ASAP1* per cell; Fig. 5*B*). The remaining case (4.5%) showed amplification of *ASAP1* (cells with gain of *ASAP1* signals relative to CEP 8 signals; Fig. 5*C*).

Effects of siRNA-reduced ASAP1 protein expression on cell migration and Matrigel invasiveness of PC-3 cells. *In vitro* scratch wound-healing and cell invasion assays were used to examine the effect of reduced ASAP1 protein expression on migration and tissue invasion of PC-3 cells. These established human prostate cancer cells, commonly used to represent advanced prostate cancer, were used because they are apparently more invasive and metastatic than, e.g., LNCaP cells (27) and were found to express ASAP1 protein more highly than LNCaP cells
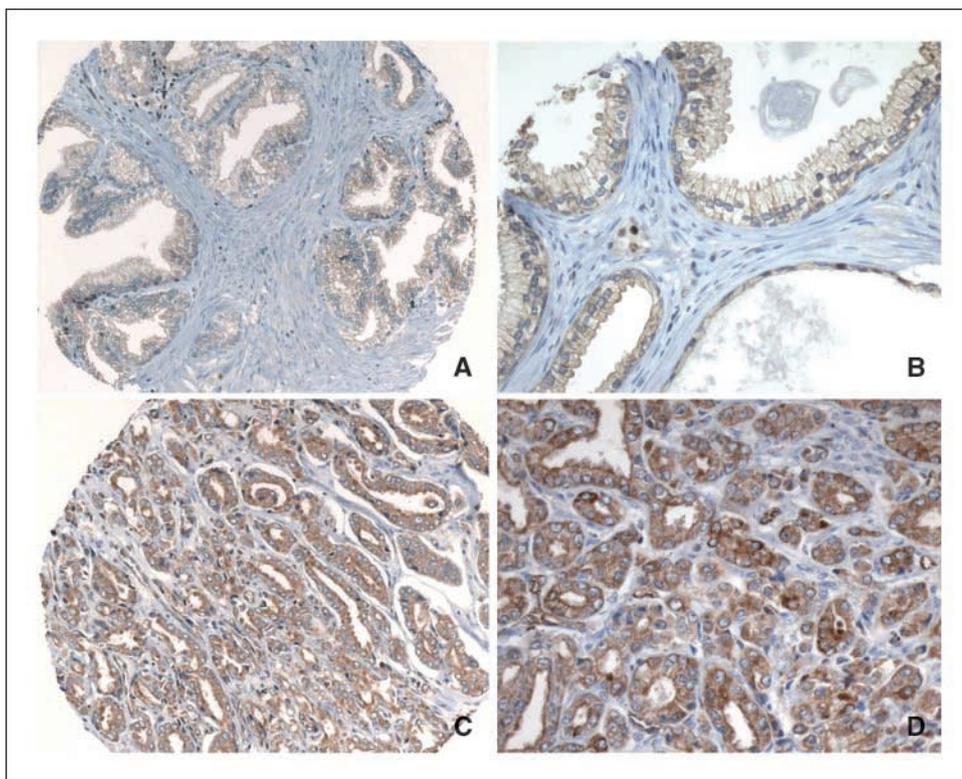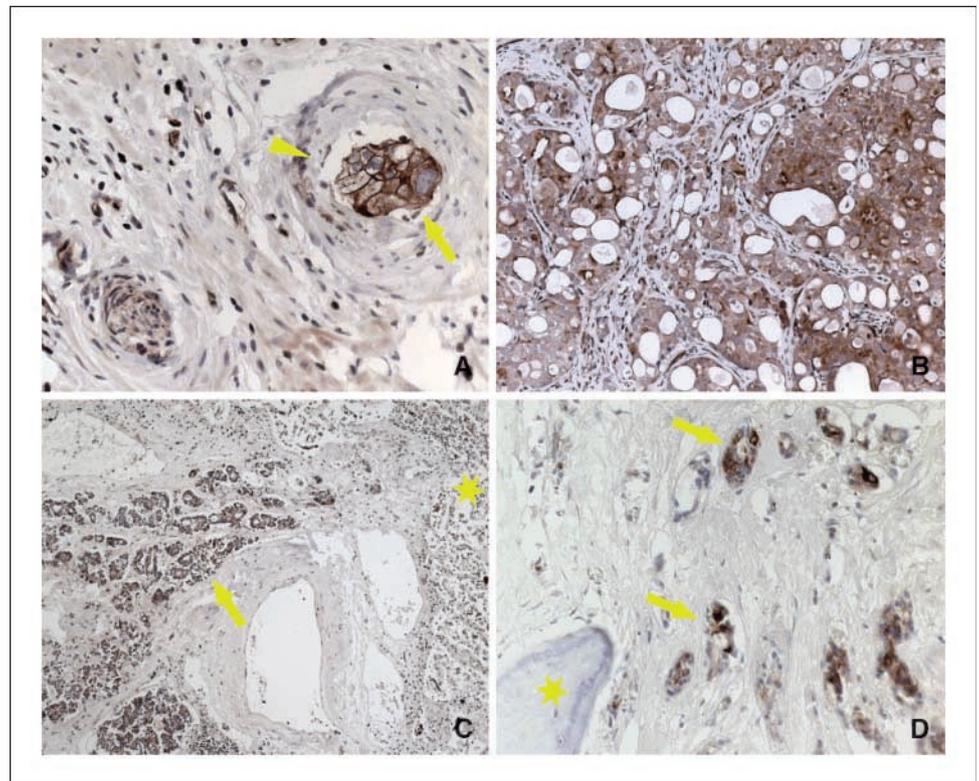
Figure 3. ASAP1 protein expression shown by immunohistochemistry in sections of clinical samples of benign and cancerous human prostate tissues. *A* and *B,* moderate plasma membrane–associated and weak cytoplasmic ASAP1 protein expression in benign prostate tissues. *C* and *D,* weak or negative plasma membrane–associated and moderate to strong cytoplasmic ASAP1 protein expression in prostate cancer cells. Original magnifications, 200× (*A* and *C*) and 400× (*B* and *D*).

Figure 4. ASAP1 protein expression shown by immunohistochemistry in sections of clinical samples of invasive and metastatic prostate cancer tissues. *A,* strong ASAP1 expression in intravascular prostate cancer cells; *arrowhead,* blood vessel. *B,* lymph node metastatic prostate cancer tissues showing very strong ASAP1 protein expression. *C,* lung metastatic prostate cancer tissue showing strong ASAP1 expression; *,* lung tissue. *D,* bone metastatic prostate cancer tissue showing very strong ASAP1 protein expression; *,* bone matrices; *arrow,* prostate cancer cells. Original magnifications, 100× (*C*), 200× (*B*), and 400× (*A* and *D*).

(Fig. 6*A*). Reduction of ASAP1 expression in PC-3 cells was obtained by transfection of the cells with *ASAP1*-targeting siRNAs. As shown by Western blot analysis, ASAP1 protein expression was markedly reduced 72 h after transfection with siRNA1 and siRNA2, in contrast to cells transfected with the vehicle (Lipofectamine 2000) or scramble siRNA (Fig. 6*B*). In the wound-healing assays, the wounded areas in the vector-treated and scramble siRNA-treated control cultures were repopulated during a 24-h period by 81.6 ± 12.7% and 76.4 ± 12.2%, respectively. In contrast, in the cultures treated with *ASAP1*-targeting siRNA1 and siRNA2, the wounded areas were repopulated by only 40.1 ± 11.2% and 40.7 ± 14.3%, respectively. The data indicate that reduction of ASAP1 protein expression markedly inhibited PC-3 cell migration by ~50% ($P < 0.01$; Fig. 6*C*). In the cell invasion assay, the siRNA-induced

reduction of ASAP1 expression resulted in a markedly lower percentage of invading cells (12.7 ± 6.2% and 12.9 ± 5.5% in siRNA1-treated and siRNA2-treated cells, respectively) compared with vector-treated (43.2 ± 3.2%) and scramble siRNA-treated (35.5 ± 3.9%) cells (Fig. 6*D*), an average reduction of ~67%. These studies show that the *ASAP1* gene has an important function in the migratory and tissue-invasive properties of PC-3 cells.

Discussion

Most deaths from prostate cancer are due to metastases that are highly resistant to conventional therapies. Thus far, few metastasis-associated genes that could be used as reliable metastatic biomarkers or therapeutic targets for better management of the disease have been discovered (2, 3, 7). The aim of the present study
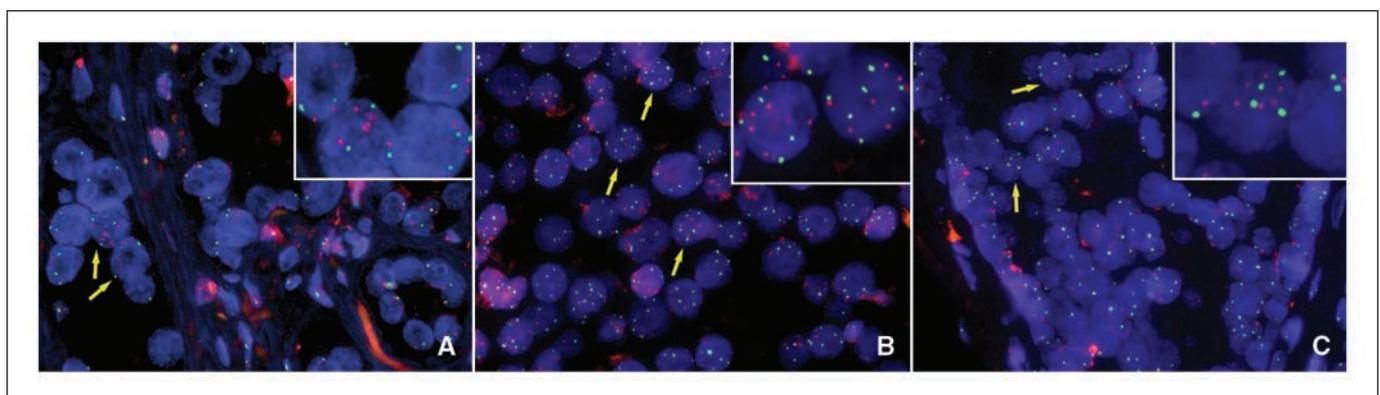

Figure 5. Gain and/or amplification of *ASAP1* shown by dual-color FISH in human primary prostate cancer tissues. *A,* nuclei showing a balanced increase in *ASAP1* gene (*red*) and chromosome 8 number (*green*) indicating low polysomic copy gain (three to four copies). *B,* nuclei showing a balanced increase in *ASAP1* gene and chromosome 8 number indicating high polysomic copy gain (five or more copies). *C,* nuclei showing an increase in *ASAP1* copies relative to chromosome 8 copies indicating *ASAP1* gene amplification. Original magnification, 400×.
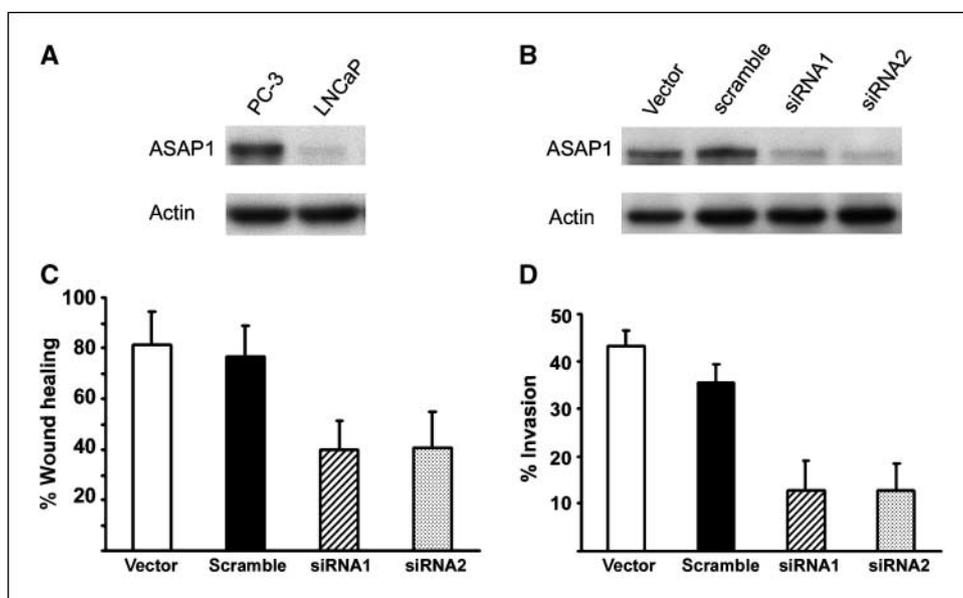
Figure 6. ASAP1 protein expression in PC-3 and LNCaP cells and siRNA-induced reduction in (*a*) cellular ASAP1 protein content and (*b*) migration and Matrigel invasion of PC-3 cells. *A,* Western blot showing ASAP1 protein expression in PC-3 and LNCaP cells. *B,* Western blot showing reduction of ASAP1 protein content in PC-3 cells transfected with either siRNA1 or siRNA2, targeting the *ASAP1* gene, in contrast to vector-treated and scramble-treated cells. *C,* repopulation of scratch-wounded areas in monolayers of siRNA-transfected and control PC-3 monolayers 24 h after scratching. *Columns,* mean; *bars,* SD. *D,* migration of siRNA-transfected and control PC-3 cells. See Materials and Methods for details.

was to identify such metastasis-associated genes on the basis of differential expression in metastatic prostate cancer relative to nonmetastatic disease. The establishment of the nonmetastatic PCa2 subline, similar to the metastatic PCa1-met subline with regard to morphology, growth rate, and SKY karyotype (Fig. 1), and derivation from the same patient's cancer allowed comparative SAGE analysis of a pair of closely related prostate cancer sublines with karyotypes that are quite close to normal. The comparison was especially significant because the sublines were grown in an identical, orthotopic microenvironment (the anterior prostate)—an important factor in the development of cancer metastasis (4, 28). This also helped to preclude differences in gene expression of the sublines due to differences in environmental factors. The finding of various differentially expressed genes previously reported to have roles in prostate cancer metastasis indicated the validity of this approach and instigated a focus on *ASAP1*, a gene that had not previously been associated with advanced prostate cancer.

The *ASAP1* (*AMAP1/DDEF1*) gene encodes an Arf GTPase-activating protein that localizes to focal adhesions and is involved in regulation of membrane trafficking and cytoskeletal remodeling (29). ASAP1 protein has been associated with metastasis in other cancers, e.g., breast cancer (14) and also melanoma (30). In the present study, we have shown that siRNA-reduced ASAP1 protein expression in cultured PC-3 human prostate cancer cells led to a marked reduction of their *in vitro* migration (~50%) and percentage of Matrigel-invading cells (~67%; Fig. 6B–D). Importantly, ASAP1 protein, as well as mRNA, was expressed at a significantly higher level in a metastatic prostate tumor subline than in a nonmetastatic subline or benign prostate tissue, all derived from the same patient (Fig. 2). Furthermore, immunohistochemistry of a series of clinical prostate cancer specimens, i.e., benign, primary, and secondary prostate cancer tissues, showed that there is a strong correlation between highly increased ASAP1 protein levels and metastasis (Figs. 3 and 4). Taken together, these findings suggest that overexpression of the *ASAP1* gene has a metastasis-promoting effect in prostate cancer.

At present, the basis for the increased ASAP1 protein expression in the prostate cancer samples examined is not clear. As shown by FISH analysis, 58% of the primary prostate cancers showed a substantial increase in *ASAP1* gene copy number per cell, mainly a result of polysomy of chromosome 8 (Fig. 5). This suggests that an increase in *ASAP1* gene copy number may, at least in part, be responsible for the elevated ASAP1 protein expression in the cancer specimens. It is of major interest that the *ASAP1* gene has been mapped to chromosomal location 8q24.21. Gain of the 8q region has been reported as one of the most common alterations in prostate cancer tissue (31–35) and has also been observed in PC-3 cells (36, 37). The increase in *ASAP1* gene copy numbers found in the majority of the prostate cancer samples examined is consistent with such an 8q gain (Fig. 5). Furthermore, the increase in metastatic activity associated with increased ASAP1 protein expression (Figs. 2–4), is consistent with reports that gain of the 8q region correlates with metastatic progression and poor prognosis of prostate cancer (38, 39).

As reported by Onodera et al. (14), elevated expression of ASAP1 protein correlated with invasiveness of breast cancer. The invasion-related action of the ASAP1 protein in this disease seems to be based on its formation of a trimeric complex with paxillin and cortactin, proteins with a pivotal role in cellular invasiveness (14). Future studies will examine whether the invasion-related activity of ASAP1 protein in prostate cancer is based on a similar mechanism. Attention will also be given to the change in localization of ASAP1 protein expression away from the plasma membrane, as observed with rapidly growing prostate cancer tissue in contrast to benign prostatic tissue (Fig. 2). Studies are ongoing in the laboratory to determine whether inhibiting expression of ASAP1 protein can lead to reduction of metastatic ability of tumors *in vivo*. Furthermore, studies will be initiated on ASAP1 expression in a wide range of primary and secondary prostate cancers with clinical outcome information.

It seems from the present study that the *ASAP1* gene may play a major role in prostate cancer metastasis. The *ASAP1* gene and/or its products (mRNA and protein) could represent potential new biomarkers and/or therapeutic targets for the disease.

Disclosure of Potential Conflicts of Interest

No potential conflicts of interest were disclosed.

Acknowledgments

References

1. Isaacs JT. New strategies for the medical treatment of prostate cancer. BJU Int 2005;96 Suppl 2:35–40.
2. Foley R, Hollywood D, Lawler M. Molecular pathology of prostate cancer: the key to identifying new biomarkers of disease. Endocr Relat Cancer 2004;11:477–88.
3. Glinsky GV, Glinskii AB, Stephenson AJ, Hoffman RM, Gerald WL. Gene expression profiling predicts clinical outcome of prostate cancer. J Clin Invest 2004;113:913–23.
4. Fidler IJ. The pathogenesis of cancer metastasis: the "seed and soil" hypothesis revisited. Nat Rev Cancer 2003;3:453–8.
5. Varambally S, Yu J, Laxman B, et al. Integrative genomic and proteomic analysis of prostate cancer reveals signatures of metastatic progression. Cancer Cell 2005;8:393–406.
6. Paris PL, Weinberg V, Simko J, et al. Preliminary evaluation of prostate cancer metastatic risk biomarkers of disease. Int J Biol Markers 2005;20:141–5.
7. Gutman S, Kessler LG. The U.S. Food and Drug Administration perspective on cancer biomarker development. Nat Rev Cancer 2006;6:565–71.
8. Voskoglou-Nomikos T, Pater JL, Seymour L. Clinical predictive value of the *in vitro* cell line, human xenograft, and mouse allograft preclinical cancer models. Clin Cancer Res 2003;9:4227–39.
9. Sharpless NE, Depinho RA. The mighty mouse: genetically engineered mouse models in cancer drug development. Nat Rev Drug Discov 2006;5:741–54.
10. Fidler IJ. Critical determinants of metastasis. Semin Cancer Biol 2002;12:89–96.
11. Wang Y, Xue H, Cutz JC, et al. An orthotopic metastatic prostate cancer model in SCID mice via grafting of a transplantable human prostate tumor line. Lab Invest 2005;85:1392–404.
12. Wang Y, Revelo MP, Sudilovsky D, et al. Development and characterization of efficient xenograft models for benign and malignant human prostate tissue. Prostate 2005;64:149–59.
13. Saha S, Sparks AB, Rago C, et al. Using the transcriptome to annotate the genome. Nat Biotechnol 2002;20:508–12.
14. Onodera Y, Hashimoto S, Hashimoto A, et al. Expression of AMAP1, an ArfGAP, provides novel targets to inhibit breast cancer invasive activities. EMBO J 2005; 24:963–73.

15. Ohl F, Jung M, Xu C, et al. Gene expression studies in prostate cancer tissue: which reference gene should be selected for normalization? J Mol Med 2005;83:1014–24.
16. Lee CH, Xue H, Sutcliffe M, et al. Establishment of subrenal capsule xenografts of primary human ovarian tumors in SCID mice: potential models. Gynecol Oncol 2005;96:48–55.
17. Cutz JC, Guan J, Bayani J, et al. Establishment in severe combined immunodeficiency mice of subrenal capsule xenografts and transplantable tumor lines from a variety of primary human lung cancers: potential models for studying tumor progression-related changes. Clin Cancer Res 2006;12:4043–54.
18. Todaro GJ, Lazar GK, Green H. The initiation of cell division in a contact-inhibited mammalian cell line. J Cell Physiol 1965;66:325–33.
19. Hendrix MJ, Seftor EA, Seftor RE, Fidler IJ. A simple quantitative assay for studying the invasive potential of high and low human metastatic variants. Cancer Lett 1987;38:137–47.
20. Gao AC, Lou W, Dong JT, Isaacs JT. CD44 is a metastasis suppressor gene for prostatic cancer located on human chromosome 11p13. Cancer Res 1997;57:846–9.
21. Bussemakers MJ, van Moorselaar RJ, Giroldi LA, et al. Decreased expression of E-cadherin in the progression of rat prostatic cancer. Cancer Res 1992;52:2916–22.
22. Umbas R, Schalken JA, Aalders TW, et al. Expression of the cellular adhesion molecule E-cadherin is reduced or absent in high-grade prostate cancer. Cancer Res 1992;52:5104–9.
23. Taichman RS, Cooper C, Keller ET, Pienta KJ, Taichman NS, McCauley LK. Use of the stromal cell-derived factor-1/CXCR4 pathway in prostate cancer metastasis to bone. Cancer Res 2002;62:1832–7.
24. Thompson TC. Metastasis-related genes in prostate cancer: the role of caveolin-1. Cancer Metastasis Rev 1998;17:439–42.
25. Zhau HE, Pisters LL, Hall MC, et al. Biomarkers associated with prostate cancer progression. J Cell Biochem Suppl 1994;19:208–16.
26. Kibel AS, Freije D, Isaacs WB, Bova GS. Deletion mapping at 12p12-13 in metastatic prostate cancer. Genes Chromosomes Cancer 1999;25:270–6.
27. Hoosein NM, Boyd DD, Hollas WJ, Mazar A, Henkin J, Chung LW. Involvement of urokinase and its receptor in the invasiveness of human prostatic carcinoma cell lines. Cancer Commun 1991;3:255–64.

28. Xu J, Wang R, Xie ZH, et al. Prostate cancer metastasis: role of the host microenvironment in promoting epithelial to mesenchymal transition and increased bone and adrenal gland metastasis. Prostate 2006;66:1664–73.
29. Randazzo PA, Hirsch DS. Arf GAPs: multifunctional proteins that regulate membrane traffic and actin remodelling. Cell Signal 2004;16:401–13.
30. Ehlers JP, Worley L, Onken MD, Harbour JW. DDEF1 is located in an amplified region of chromosome 8q and is overexpressed in uveal melanoma. Clin Cancer Res 2005;11:3609–13.
31. Visakorpi T, Kallioniemi AH, Syvanen AC, et al. Genetic changes in primary and recurrent prostate cancer by comparative genomic hybridization. Cancer Res 1995;55:342–7.
32. Yeager M, Orr N, Hayes RB, et al. Genome-wide association study of prostate cancer identifies a second risk locus at 8q24. Nat Genet 2007;39:645–9.
33. Haiman CA, Patterson N, Freedman ML, et al. Multiple regions within 8q24 independently affect risk for prostate cancer. Nat Genet 2007;39:638–44.
34. Gudmundsson J, Sulem P, Manolescu A, et al. Genome-wide association study identifies a second prostate cancer susceptibility variant at 8q24. Nat Genet 2007;39:631–7.
35. Kim JH, Dhanasekaran SM, Mehra R, et al. Integrative analysis of genomic aberrations associated with prostate cancer progression. Cancer Res 2007;67: 8229–39.
36. Tsuchiya N, Kondo Y, Takahashi A, et al. Mapping and gene expression profile of the minimally overrepresented 8q24 region in prostate cancer. Am J Pathol 2002;160:1799–806.
37. Porkka KP, Tammela TL, Vessella RL, Visakorpi T. RAD21 and KIAA0196 at 8q24 are amplified and overexpressed in prostate cancer. Genes Chromosomes Cancer 2004;39:1–10.
38. van Dekken H, Alers JC, Damen IA, et al. Genetic evaluation of localized prostate cancer in a cohort of forty patients: gain of distal 8q discriminates between progressors and nonprogressors. Lab Invest 2003;83: 789–96.
39. Ribeiro FR, Jeronimo C, Henrique R, et al. 8q gain is an independent predictor of poor survival in diagnostic needle biopsies from prostate cancer suspects. Clin Cancer Res 2006;12:3961–70.